Surface-related multiple leakage extraction using local primary-and-multiple orthogonalization

Zhang, Dong; Verschuur, D. J.Eric; Qu, Shan; Chen, Yangkang

DOI
10.1190/geo2019-0465.1

Publication date
2020

Document Version
Final published version

Published in
Geophysics

GEOPHYSICS, VOL. 85, NO. 1 (JANUARY-FEBRUARY 2020); P. V81–V97, 21 FIGS.
10.1190/GEO2019-0465.1

Surface-related multiple leakage extraction using local primary-and-multiple orthogonalization

Dong Zhang[1], D. J. (Eric) Verschuur[1], Shan Qu[1], and Yangkang Chen[2]

ABSTRACT

Accurate multiple removal remains an important step in seismic data processing sequences. Most multiple removal methods, such as surface-related multiple elimination (SRME), consist of a multiple prediction step and an adaptive subtraction step. Due to imperfect circumstances (e.g., coarse data sampling) or built-in assumptions (e.g., 2D method versus 3D data), multiple leakage is commonly observed in the results. More aggressive adaptive multiple subtraction can reduce the leakage problem, for example, by using small local windows and a long filter length, but at the risk of severely damaging the primaries due to overfitting. In contrast, conservative adaptive subtraction with large or global windows and a short filter length can preserve most primary energy while tending to have more multiple leakage because of underfitting. Assuming that the primaries and multiples do not correlate locally in the time-space domain, our solution to this problem is to extract the leaked multiples from the initially estimated primaries using local primary-and-multiple orthogonalization (LPMO) rather than restoring the damaged primaries. Our framework consists of two steps: an initial primary estimation step and a multiple leakage extraction step. The initial step corresponds to conservative SRME (or an equivalent method) that produces the initially estimated primary and multiple models. The second step is based on LPMO to retrieve the leaked multiples from the estimated primaries via a time- and space-varying weight function that is estimated from the local correlation of predicted multiples and residual multiples in the estimated primaries with the help of shaping regularization. In this way, we can obtain a better primary model that has much less leaked multiple energy and less primary damage at the same time. We find good performance of our framework via two synthetic data examples and one field data example.

INTRODUCTION

Surface-related multiples have been regarded as coherent noise and removed before the subsequent processing workflows for decades (Ryu, 1982; Hampson, 1986; Verschuur and Berkhout, 1997; Weglein et al., 1997; Chen et al., 2017). Meanwhile, exploration geophysicists gradually realized that these multiples (note that we refer to multiples as only surface-related multiples in this paper and that internal multiples are beyond the scope of this research) are able to see through the earth multiple times and, therefore, carry valuable physical information about the subsurface (Verschuur, 2006). Multiples are treated nowadays as useful signals as well and can be directly included into imaging algorithms (Brown and Guitton, 2005; Zhang and Schuster, 2013; Lu et al., 2015; Davydenko and Verschuur, 2017, 2018; Nath and Verschuur, 2017). Although full wavefield imaging (including primaries and all types of multiples) can be achieved, it is still desired to estimate primaries and multiples first and then image them separately, due to the crosstalk of multiples during imaging, the challenges in shallow-water scenarios, and the benefits for conventional primary-oriented processing.

Surface-related multiple elimination (SRME) has already been proved to be a powerful tool for primary and multiple estimation with the help of its data-driven engine and the strong physics behind it (Verschuur et al., 1992; Berkhout and Verschuur, 1997). Specifically, SRME first predicts the multiples based on a multidimensional convolution process from the data themselves without any prior knowledge about the subsurface and then it adaptively subtracts the predicted multiples from the original data using the minimum-energy criterion (Verschuur and Berkhout, 1997). Moreover, a full-waveform inversion-based primary and multiple estimation

Manuscript received by the Editor 23 July 2019; revised manuscript received 11 September 2019; published ahead of production 16 October 2019; published online 28 November 2019.
[1]Delft University of Technology, Department of Imaging Physics, Lorentzweg 1, 2628CJ, Delft, The Netherlands. E-mail: d.zhang-3@tudelft.nl (corresponding author); d.j.verschuur@tudelft.nl; s.qu@tudelft.nl.
[2]Zhejiang University, School of Earth Sciences, Hangzhou, China. E-mail: yangkang.chen@zju.edu.cn.

scheme is proposed by van Groenestijn and Verschuur (2009a, 2009b), which is known as estimation of primaries by sparse inversion (EPSI). Lin and Herrmann (2013) further propose a robust version of EPSI based on $L1$-norm minimization. Concretely, the multiple prediction and adaptive subtraction process is replaced by a full-waveform inversion process, in which the primary impulse response and source wavelet are the unknowns. Another inversion approach called closed-loop SRME (CL-SRME) with different parameterization, being the primary and surface operator, is proposed by Lopez and Verschuur (2014, 2015), and it combines the robustness of SRME with EPSI. Although the inversion schemes enjoy more physical consistency, they lack computational efficiency, which is the bottleneck for wide industry application. SRME, in many cases, will still be the preferable choice in terms of computational cost.

Among all of the difficulties of SRME, surface-related multiple leakage is a long-standing problem for primary and multiple estimation (Verschuur, 2006). The leaked multiple energy will undoubtedly damage the subsequent migration and interpretation accuracy. Furthermore, this leaked energy is even more challenging for the already difficult shallow-water scenario due to the strong impact of missing near offsets (Hargreaves, 2006; van Groenestijn and Verschuur, 2009a, 2009b; Jin and Wang, 2012; Hung et al., 2014; Kostov et al., 2015; Lopez and Verschuur, 2015; Zhang and Verschuur, 2019). Multiple prediction and adaptive subtraction are indispensable ingredients for SRME, and both of them could lead to the multiple leakage issue. In fact, multiple prediction is the most robust part of SRME because of its fulfillment of strong physics, but it still requires densely sampled data (near-offset data for the 2D situation and undersampling in the crossline direction with near offsets missing for 3D data), which is always difficult to satisfy in the real world (Dragoset and Jericevic, 1998). Otherwise, the sampling issue results in phase and amplitude errors for the predicted multiples. Thus, with the inaccurate predicted multiple model, it is more likely to limit the performance of adaptive subtraction and leave some amount of multiple leakage afterward. Much effort on data interpolation is spent to feed densely sampled data to SRME. Kabir and Verschuur (1995) propose to restore the missing offsets with the parabolic Radon transform based on partial normal moveout corrected common-midpoint gathers. Interferometric interpolation methods are also available and are effective for 2D cases (Wang et al., 2009; Hanafy and Schuster, 2014). Van Dedem and Verschuur (2005) introduce a sparse inversion interpolation approach for 3D surface-related multiple prediction. Van Groenestijn and Verschuur (2009a) present an EPSI-based approach to reconstruct near-offset data by using multiples. Dragoset et al. (2010) describe on-the-fly interpolation for 3D SRME application. Lopez and Verschuur (2015) propose to use the focal domain constraint to interpolate missing data within the CL-SRME framework. Zhang and Verschuur (2019) propose to use the data reconstruction power of full wavefield migration as a better input for CL-SRME.

Adaptive subtraction, on the other hand, is the most problematic step in SRME, or other prediction and subtraction methods, due to its harsh assumption that primaries and multiples should not correlate anywhere. Multiple leakage occurs when primaries and multiples partially correlate, which is usually unavoidable. The core of adaptive subtraction is estimating a matching filter to correct for the amplitude and phase distortions. Spitz (1999) indicates the pitfalls of the $L2$-norm adaptive subtraction process in which some part of the multiples is not orthogonal to the primaries. Many researchers have reported different approaches to improve the adaptive subtraction by relaxing its original assumption or replacing it. Guitton and Verschuur (2004) propose to use $L1$-norm instead of $L2$-norm adaptive subtraction when the primaries are much stronger than the multiples. Building on the work of Spitz (1999), Guitton (2005) shows on field data that the pattern-based subtraction method is less sensitive to the overlap between primaries and multiples; however, this method has difficulties when multiples and primaries are parallel to each other (Verschuur, 2006). Fomel (2009) proposes regularized nonstationary regression-based adaptive subtraction without breaking the data into local windows. Xue et al. (2016) introduce a nonlinear adaptive multiple subtraction method using the amplitude-preserving high-order sparse Radon transform. Hermann and Verschuur (2004) present a sparse curvelet-domain subtraction approach by iteratively shrinking the curvelet coefficients. Attracted by its effectiveness, several extended curvelet-based techniques are proposed (Hermann et al., 2008; Wang et al., 2008; Neelamani et al., 2010). However, the computational efficiency is currently the main drawback of curvelet-based methods, and they also suffer the risk of dimming primaries while removing multiples. In addition to the marine acquisition, Kelamis and Verschuur (2000) introduce a very detailed and much more difficult application of the adaptive multiple subtraction for land seismic data.

Despite all of the efforts mentioned above, surface-related multiple leakage can still be seen in the results of SRME-predicted primaries. The reasons behind this are, first, the data reconstruction can never be perfect, which leads to phase and amplitude errors in the predicted multiples. Second, the assumption of adaptive subtraction that primaries and multiples do not correlate is often not met. Essentially, the imperfections of adaptive subtraction directly lead to multiple leakage in the estimated primaries. It tends to be either underfitting or overfitting for the subtraction step regardless of the forced constraint. Underfitting results in more severe multiple leakage, whereas overfitting can alleviate multiple leakage to some extent. However, overfitting is unfortunately the main cause for primary energy damage because removing more multiples usually comes along with damaging primaries. The ability of least-squares adaptive subtraction strongly depends on the size of local windows and the filter length. A small window size and a long filter length, which is called standard SRME in this paper, lead to better multiple removal, but at the same time cause more primary damage. For primary-oriented processing, the best one can achieve during the trade-off is to protect the primaries as much as possible and, as a result, leave some amount of multiple leakage. That is, the local windows for SRME should be relatively large and the filter length for adaptive subtraction should be relatively short. We call this type of SRME conservative SRME. More specifically, note that in this paper, conservative SRME indicates the $L2$-norm adaptive subtraction step in the last iteration with large local windows or even global windows and a short filter length, in which the primaries are not damaged, whereas surface-related multiple leakage is relatively more severe. In contrast, standard SRME means the $L2/L1$-norm adaptive subtraction step in the last iteration with small local windows and a long filter length, in which the multiple leakage is alleviated, whereas the primary damage is relatively more severe. Instead of solving the leakage issue within SRME itself, it might be much easier and more effective if another external extraction step is included after conservative SRME to compensate for multiple leakage.

To this end, multiple leakage can also be seen as one type of signal leakage if we temporarily treat multiples as our useful signal.

Signal leakage is a long-standing problem in the field of random noise attenuation (Gülünay, 2017; Chen et al., 2018). Most studies try to propose more advanced denoising algorithm by introducing more solid assumptions. However, the fact that signal leakage always exists should be kept in mind regardless of the algorithms. An extra external step to compensate for signal leakage might therefore be preferable. Chen and Fomel (2015) propose to extract the leaked signal from random noise using an extra local signal-and-noise orthogonalization step and show very promising results, in which traditional f-x deconvolution is used as the initial denoising operator. In addition, successful applications on removing ground-roll noise and blending noise based on local orthogonalization are reported (Chen et al., 2015: Chen, 2015). Inspired by the concept of local orthogonalization, we propose a new framework for primary estimation and surface-related multiple leakage extraction using local primary-and-multiple orthogonalization (LPMO) to complement conservative SRME. This local orthogonalization assumption is equivalent to assuming that the primaries and multiples do not correlate locally in the time-space domain. In this paper, we focus on standard and conservative SRME with least-squares adaptive subtraction. The proposed framework mainly consists of two steps: an initial primary estimation step and a multiple leakage extraction step. The initial step corresponds to the conservative SRME (or an equivalent method), which produces the initially estimated primary and multiple models. The second step is based on LPMO to extract the leaked multiples from the estimated primaries via a time- and space-varying weight function that is estimated from the local correlation of predicted multiples and residual multiples in the estimated primaries with the help of shaping regularization, which can be regarded as an external remedy for correcting the initially predicted primaries and multiples from conservative SRME. Thus, we can obtain better primary and multiple models for subsequent processing steps. Preliminary results are shown in Zhang et al. (2019a). Fair comparisons with standard SRME are also provided to display their different behaviors in this paper. We demonstrate the good performance of our proposed two-step framework on two synthetic and one field data set. Above all, the proposed framework could make the conventional adaptive subtraction process easier to parameterize and could also be beneficial for the subsequent quality control (QC) step.

We organize this paper as follows: First, we present a brief review of SRME and some important aspects for adaptive subtraction. The LPMO is then introduced in detail, which together with a conservative SRME primary estimation approach forms our proposed two-step framework. Two synthetic examples are provided to describe and compare the proposed approach with standard SRME. In addition, a comprehensive investigation on shallow-water field data is presented to demonstrate the effectiveness of the proposed framework. A discussion part on the important aspects of the algorithm is also included at the end.

REVIEW OF SRME

SRME or specifically iterative SRME is briefly reviewed in this section. Let $\mathbf{P}$ represent the monochromatic total upgoing wavefields from all sources recorded at the surface and $\mathbf{P}_0$ denote the primary wavefields. The terms $\mathbf{P}_0$ and $\mathbf{P}$ are in the detail-hiding notation (Berkhout, 1982), where vectors (the columns of the matrix) represent monochromatic shot records. The core engine used for all SRME-based algorithms can be expressed as follows:

$$\mathbf{P}_0 = \mathbf{P} - \mathbf{P}_0\mathbf{A}\mathbf{P} = \mathbf{P} - \mathbf{M}, \tag{1}$$

where $\mathbf{A}$ is the surface operator, being defined as $\mathbf{S}^{-1}\mathbf{R}^{\cap}$, i.e., the surface reflectivity from below combined with the inverse source properties. Surface multiples $\mathbf{M}$ can be predicted based on $\mathbf{P}_0\mathbf{A}\mathbf{P}$. Traditional SRME based on equation 1 is an iterative approach (Berkhout and Verschuur, 1997) in the way that $\mathbf{P}_0^{k+1} = \mathbf{P} - \mathbf{P}_0^k\mathbf{A}^{k+1}\mathbf{P}$, where k represents the iteration number, which is typically 2 or 3.

The adaptive subtraction step for SRME is implemented in the time domain using a minimum-energy constraint:

$$\mathbf{E} = \sum_{t,x_r,x_s} [p(t,x_r,x_s) - a^{(k+1)}(t) * \hat{m}^{(k+1)}(t,x_r,x_s)]^2, \tag{2}$$

where $p(t,x_r,x_s)$, $\hat{m}^{(k+1)}(t,x_r,x_s)$, and $a^{(k+1)}(t)$ represent the total upgoing wavefields, the unadapted multiples (i.e., $-\mathbf{P}_0\mathbf{P}$), and the surface operator in the time domain, respectively. The length of the surface operator is also known as the filter length, which is capable of controlling the trade-off between underfitting and overfitting. The terms x_r and x_s are the source and receiver locations of seismic data. For the standard SRME, the predicted multiples are first matched and subtracted in a global window during the first one or two iterations. Small local windows and a long filter length are then used for adaptive subtraction in the last iteration to better remove the multiples (Verschuur and Berkhout, 1997). It is worth noting that small local windows and a long filter length for standard SRME can damage the primaries, although more multiples are removed due to overfitting. On the other hand, for conservative SRME when the last iteration of adaptive subtraction is still implemented in a global window or large local windows with a short filter length, it leads to a more conservative result with much less primary damage and relatively more multiple leakage due to underfitting. However, we suggest and use conservative SRME for primary-oriented processing to avoid hurting the primaries, although there is more multiple leakage. Then, the leaked multiples can be further extracted by the algorithm discussed in the next section.

LPMO

The proposed LPMO should directly follow the initial primary and multiple estimation step and can be regarded as an external remedy for correcting the initially predicted primaries and multiples from conservative SRME. Now, we rewrite the initial estimated primary and multiple relation in the time domain using the vector notation:

$$\mathbf{p} = \mathbf{p}_0 + \mathbf{m}, \tag{3}$$

where $\mathbf{p}$ is the total upgoing wavefield. The terms $\mathbf{p}_0$ and $\mathbf{m}$ represent the initial estimated primaries and multiples using any prediction method (conservative SRME in this paper), respectively. Based on the assumption that the final estimated primaries $\tilde{\mathbf{p}}_0$ and multiples $\tilde{\mathbf{m}}$ should be orthogonal, we are capable of orthogonalizing them by

$$\tilde{\mathbf{m}} = \mathbf{m} + \mathbf{w} \circ \mathbf{m}, \tag{4}$$

$$\tilde{\mathbf{p}}_0 = \mathbf{p}_0 - \mathbf{w} \circ \mathbf{m}, \tag{5}$$

where $\mathbf{w}$ is the LPMO weight and $\circ$ denotes the Hadamard product (i.e., sample-by-sample multiplication). This local orthogonalization assumption is equivalent to assuming that the primaries and multiples do not correlate locally in the time-space domain:

$$\sum \tilde{\mathbf{p}}_0 \circ \tilde{\mathbf{m}} \approx 0. \tag{6}$$

The LPMO weight can be estimated by solving the following unconstrained minimization problem:

$$\min_{\mathbf{w}} \|\overbrace{\mathbf{p} - \mathbf{m}}^{\mathbf{p}_0} - \mathbf{w} \circ \mathbf{m}\|_2^2. \tag{7}$$

The above minimization problem uses weighted multiples to match the leaked multiples in the initially estimated primary model in a least-squares sense. By forcing a smooth constraint to the unconstrained minimization problem in equation 7, we thus obtain a constrained optimization problem:

$$\hat{\mathbf{w}} = \arg\min_{\mathbf{w}} \|\mathbf{p}_0 - \mathcal{M}\mathbf{w}\|_2^2 + \mathbf{S}(\mathbf{w}), \tag{8}$$

where $\mathcal{M} = \mathrm{diag}(\mathbf{m})$ and $\mathbf{S}(\mathbf{w})$ denotes a smooth constraint operator. Furthermore, with the power of shaping regularization (Fomel, 2007b), we are able to solve the least-squares problem:

$$\hat{\mathbf{w}} = [\lambda^2 \mathbf{I} + \mathcal{T}(\mathcal{M}^T\mathcal{M} - \lambda^2 \mathbf{I})]^{-1} \mathcal{T}\mathcal{M}^T \mathbf{p}_0, \tag{9}$$

where λ is a scaling parameter and $\mathcal{T}$ represents a triangle smoothing operator that fulfills the role of a smooth constraint operator $\mathbf{S}(\mathbf{w})$. The symbol $[\cdot]^T$ denotes the matrix transpose. To make our solution more stable and to avoid unphysical results, we apply an additional thresholding operator and median filter to the estimated LPMO weight:

$$\bar{\mathbf{w}} = \mathbf{FT}(\hat{\mathbf{w}}), \tag{10}$$

where $\mathbf{T}$ is a thresholding operator that forces the weight to have values within 0 to 1 and $\mathbf{F}$ is a median filtering operator. The current LPMO weight range is very robust, and a more detailed description will be shown in the "Discussion" section. Therefore, we can substitute our final estimated weight $\bar{\mathbf{w}}$ back into equations 4 and 5 to obtain the final results.

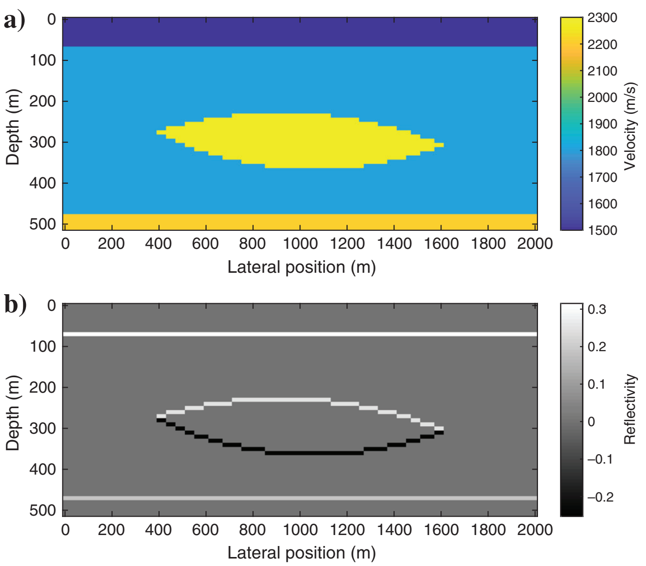

Figure 1. A 2D lens-shaped synthetic model. (a) Velocity model. (b) Reflectivity model.

RESULTS

We have investigated our proposed two-step framework on two synthetic data sets and one field data set. For all the examples, a conservative SRME followed by the LPMO is applied to obtain the best result. In contrast, we also provide the standard SRME results as the comparison.

Lens-shaped synthetic data example

We first test our proposed two-step framework, namely conservative SRME followed by LPMO, on a 2D synthetic lens-shaped model, which consists of a water layer, a high-velocity lens-shaped body overlying a target layer. The sources and receivers are placed covering the whole surface with a lateral interval of 20 m. For this 2D synthetic model, full wavefield numerical data are produced using full wavefield modeling (FWMod) (Berkhout, 2014) based on the velocity model in Figure 1a and the reflectivity model in Figure 1b. Figure 2 presents the modeled ground-truth wavefields, in which the true multiples and primaries are used as reference data.

Initially predicted multiples and primaries using conservative SRME with a global subtraction window are displayed in Figure 3a and 3b, respectively. The filter length for the global adaptive subtraction is 28 ms. Note that due to some overlapping energy between multiples and primaries and global window adaptive subtraction, there exists obvious multiple leakage in the initially estimated primary model shown in Figure 3b. In addition, the amplitude of the estimated multiples in Figure 3a is weaker than the true multiples in Figure 2b due to this leakage. However, these leaked multiples can be well detected by the proposed LPMO where in this example, the smoothing radius of the triangle smoothing operator is 2 time samples, the thresholding ranges from 0 to 1, and the size of the median filter is 5 time samples $*$ 5 traces. The final estimated LPMO weight according to equation 10 is shown in Figure 3c. We can clearly recognize the shape of leaked multiples from the estimated weight. Thus, we use the estimated LPMO weight to extract the leaked multiple energy. After LPMO, the final estimated multiples and primaries are presented in Figure 4. Figure 4a and 4b are exactly the same conservative SRME results as Figure 3a and 3b, and they are only used for a better comparison. The most obvious multiple leakage spots indicated by the yellow arrows are successfully extracted in the final primary model as shown in Figure 4e. At the same time, we can also observe the final estimated multiples in Figure 4d extract back their leaked energy; thus, they are now more accurate and close to the true multiples in Figure 2b. To test the improvement of our proposed framework, we propose to use the so-called local similarity map (Fomel, 2007a) as an effective measure to evaluate the surface-related multiple leakage extraction performance. After calculating the local similarity between estimated primaries and multiples before and after LPMO, we are able to better judge whether the surface-related multiple leakage is extracted or not. A high similarity value means a high correlation between the two data sets. From the local similarity maps, shown in Figure 4c and 4f, it can be concluded that the leaked multiple energy at approximately 0.2 and

0.6 s has been successfully extracted due to the low similarity observed around these areas after LPMO. At the same time, it is worth noting that there still exist some high-similarity areas between the final predicted multiples and primaries after the proposed LPMO step in Figure 4f. The reason for this is that these high-similarity areas indicate the local overlapping areas between multiples and primaries. Although the overlapping areas cannot be solved due to the violation of the initial assumption, they are well protected from damage by the proposed method through the thresholding process and the smoothing operator. We also provide a single-trace comparison at offset −60 m in Figure 5. The black line denotes the modeled true primaries. The green and red lines represent the conservative SRME primaries and the primaries after LPMO, respectively. It is clear that the leaked multiples visible in the green line are effectively extracted and the red line is closer to the true primaries.

Next, we will introduce a fair comparison between the proposed framework and the standard SRME. In detail, we provide two

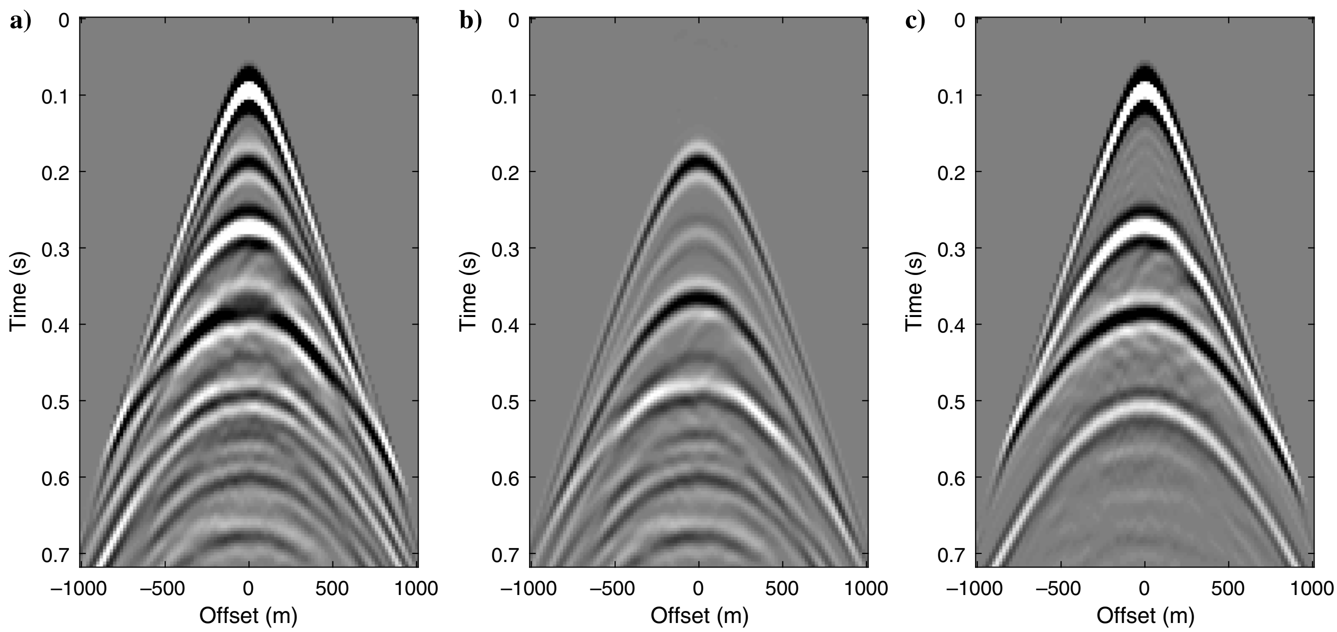

Figure 2. Modeled reference data. (a) True full wavefield. (b) True multiples. (c) True primaries.

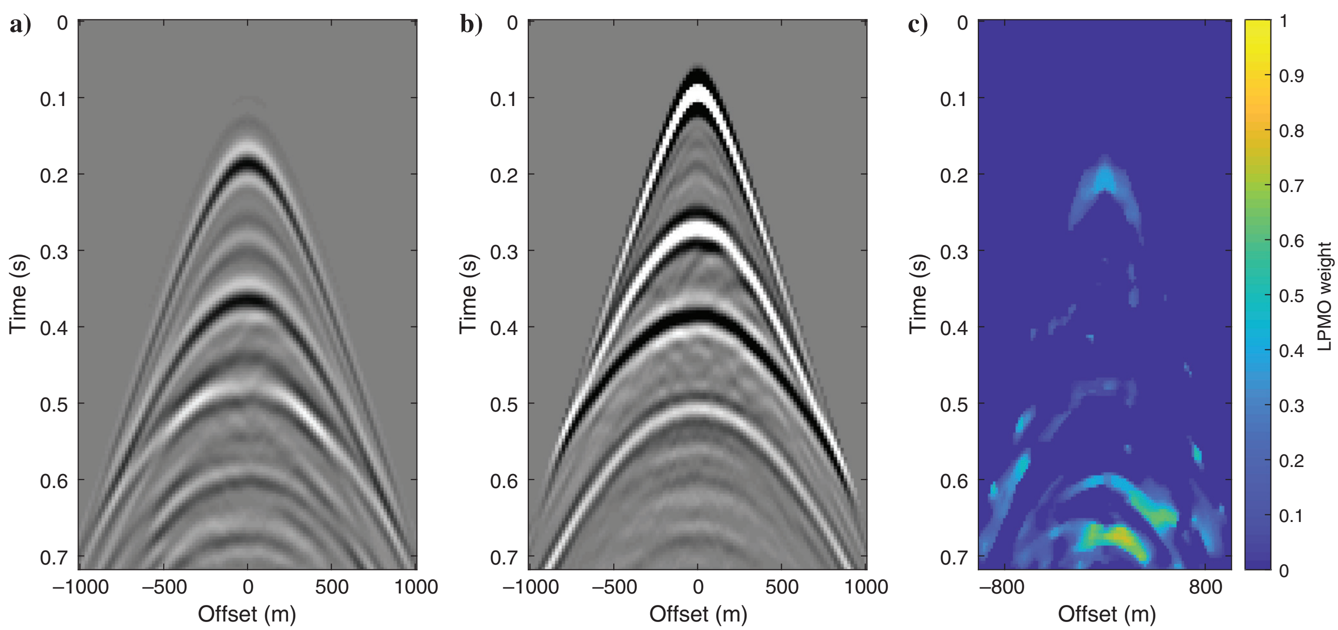

Figure 3. Initially predicted (a) multiples and (b) primaries using conservative SRME with a global subtraction window. (c) The estimated LPMO weight based on (a and b). The surface-related multiple leakage can be effectively detected by the LPMO weight.

standard SRME results: the $L2$-norm standard SRME with a 240 ms $*$ 25 traces local subtraction window size and the $L1$-norm standard SRME with a 240 ms $*$ 25 traces local subtraction window size (Guitton and Verschuur, 2004). The filter length for local subtraction windows is 28 ms. Although this filter length is the same as the global subtraction window case, it is actually much more powerful due to the use of small local windows. The estimated primary results are shown in Figure 6a and 6b, respectively. For comparison, the final estimated primaries from the proposed framework are also displayed in Figure 6c. From Figure 6, we can see that compared to the proposed primaries, the $L2$-norm and $L1$-norm standard SRME results exhibit more multiple leakage indicated by the yellow arrows and at the same time more primary damage indicated by the red arrows. Note that the $L1$-norm result seems to be slightly better than the $L2$-norm result in terms of preserving primaries, and it is also better at extracting multiple leakage at approximately 0.2 and 0.6 s. Essentially, small local subtraction windows and a long filter length in standard SRME lead to more primary damage for the adaptive subtraction although the multiple leakage of standard SRME is better than the conservative SRME result. The proposed two-step framework to extract surface-related multiple leakage, however, exhibits less primary damage and less multiple leakage.

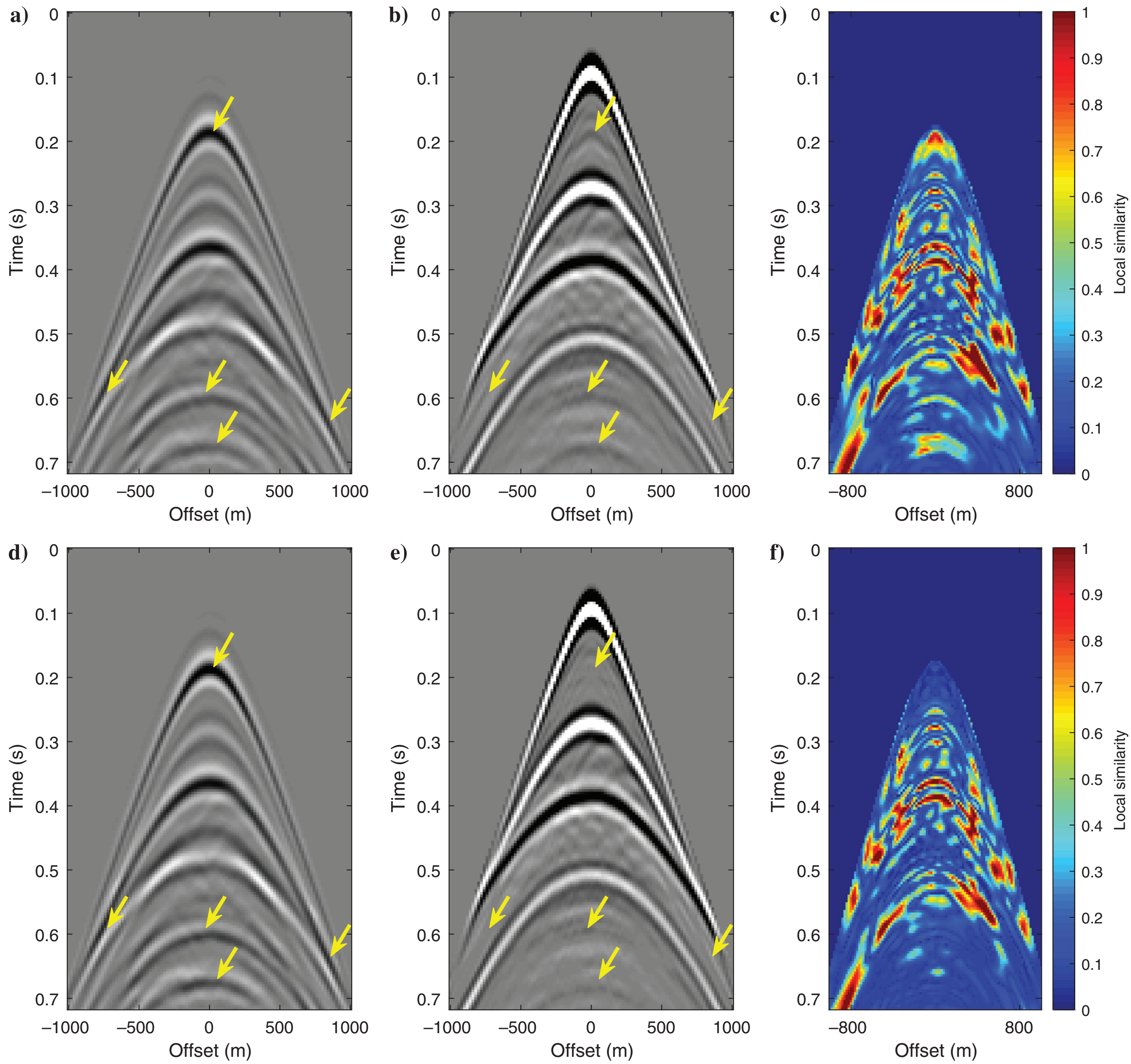

Figure 4. (a and b) Initially predicted multiples and primaries using conservative SRME with a global subtraction window, respectively. (d and e) Final estimated multiples and primaries after LPMO, respectively. (c and f) Local similarity maps before and after LPMO, respectively. The yellow arrows indicate where the leaked multiples are extracted.

Complex salt synthetic data example

The second synthetic example is a more complex salt model, which has 201 shots and 201 receivers with a lateral interval of 15 m. The velocity model is shown in Figure 7, and it consists of a shallow water layer, shallow layers, a high-velocity salt layer, and deep target layers. The data set is generated by acoustic finite-difference modeling. Figure 8a and 8b show the true full wavefield and the reference primaries, respectively. It is obvious that the surface-related multiples are strong and the deep primaries are severely interfered by the multiples. Note that the amplitude of the primaries in the full wavefield is slightly smaller than the reference primaries due to the deghosting process that was applied to the full wavefield.

The proposed two-step framework is applied to this data set. Initially estimated multiples and primaries by the conservative SRME with a global subtraction window are displayed in Figure 9a and 9b, respectively. The filter length is 40 ms. Compared to the reference primaries in Figure 8b, the multiple leakage is very obvious in the initially estimated primary model. Figure 9c demonstrates the final estimated LPMO weight that shows a good correlation to the leaked multiples. In this example, the smoothing radius of the triangle smoothing operator is 2 time samples, the thresholding ranges from −0.5 to 0.8, and the size of the median filter is 5 time samples ∗ 5 traces. Interestingly, the negative weight in this example means that there exist phase-shift errors during conservative SRME; therefore, this part of the leaked multiple needs to be extracted by negative weights. Figure 10 displays the surface-related multiple leakage extraction results before and after LPMO. The conservative SRME-predicted multiples and primaries shown in Figure 10a and 10b are only displayed for better comparison. The final estimated primaries after LPMO are presented in Figure 10e, in which the leaked multiples are extracted, indicated by yellow arrows. The black arrows indicate the extracted multiple leakage with phase-shift errors. In addition, the final estimated multiples in Figure 10d show the restoration of leaked energy compared to that in Figure 10a. Similarly, the local similarity maps in Figure 10c and

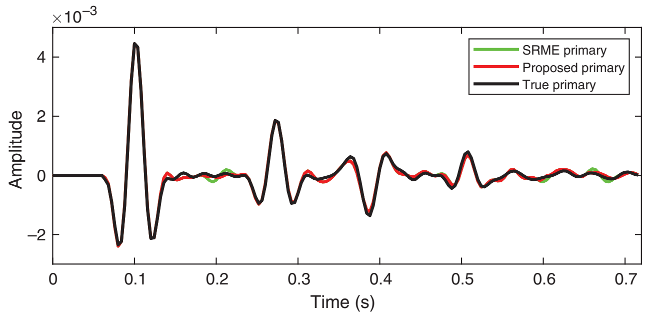

Figure 5. Single-trace comparison before and after LPMO. The black line denotes the true modeled primaries, the green line denotes the conservative SRME primaries, and the red line denotes the proposed primaries after LPMO.

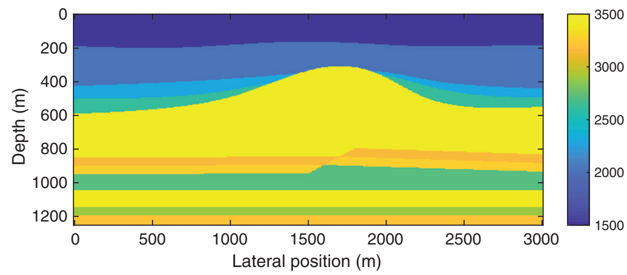

Figure 7. Complex salt velocity model.

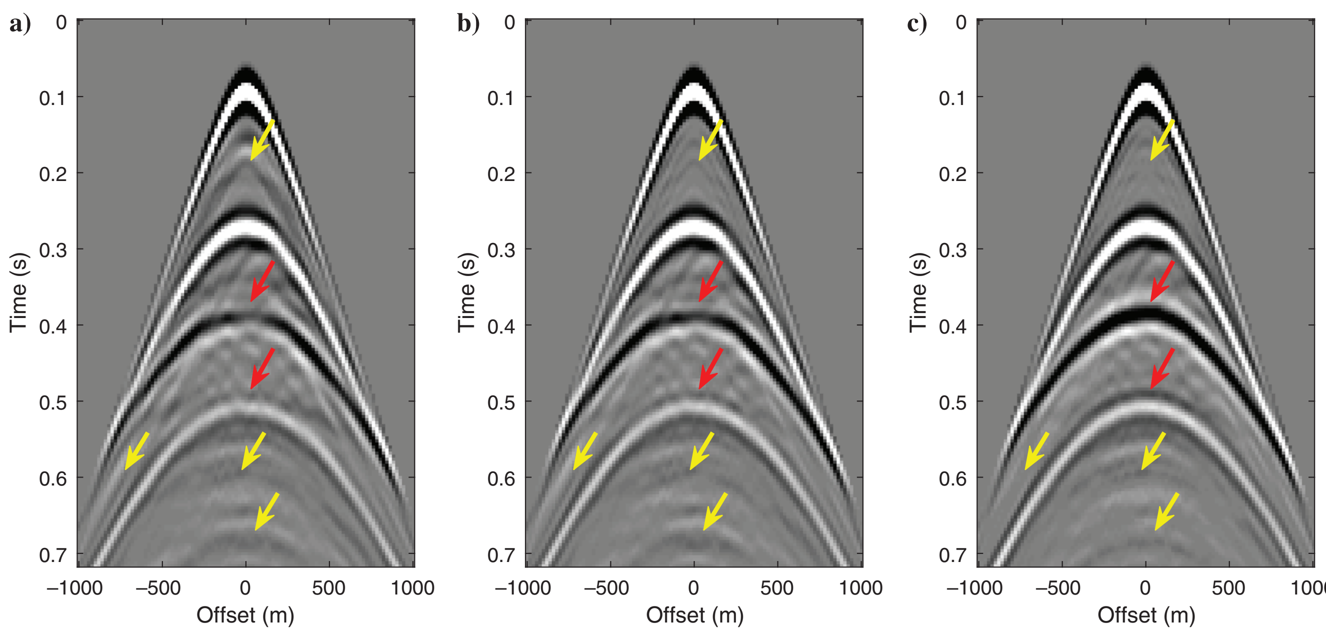

Figure 6. Comparison to the standard SRME. (a) $L2$-norm standard SRME primaries with a 240 ms ∗ 25 traces local subtraction window size. (b) $L1$-norm standard SRME primaries with a 240 ms ∗ 25 traces local subtraction window size. (c) The proposed primaries after LPMO (for comparison purposes). The yellow arrows in (a and b) denote the more severe multiple leakage compared to those in (c). The red arrows in (a and b) denote the primary damage compared to those in (c).

10f are used to better demonstrate the multiple leakage extraction improvement before and after LPMO. Moreover, a single-trace comparison at offset 0 m as shown in Figure 11 is provided to display the effect of the proposed framework in detail. The black line indicates the reference primaries, the green line indicates the conservative SRME estimated primaries, and the red line indicates the primaries from the proposed two-step framework. It can be seen that these primaries (the red line) are closer to the reference primaries (the black line) and the larger amplitude of the leaked multiples (the green line) at approximately 0.6 s can be easily misinterpreted as primary energy.

A fair comparison with the standard SRME is carried out, and it is shown in Figure 12. The $L2$-norm and $L1$-norm standard SRME primaries with a 320 ms $*$ 25 traces local subtraction window size are shown in Figure 12a and 12b, respectively. The filter length for the $L2$- and $L1$-norm cases is 56 ms, which is longer than the global subtraction case. For better comparison, our proposed two-step framework primaries are presented in Figure 12c. Compared to our proposed primaries, the yellow arrows indicate more leaked multiples in Figure 12a and 12b. However, in terms of the amount of multiple leakage, the standard SRME results all seem better than the conservative SRME result in Figure 10b due to overfitting. Meanwhile, the red arrows in the standard SRME results denote more primary damage than the proposed primaries, which is the main drawback of the standard SRME. Still, we can find that the $L1$-norm standard result seems better than the $L2$-norm standard result with respect to primary preservation.

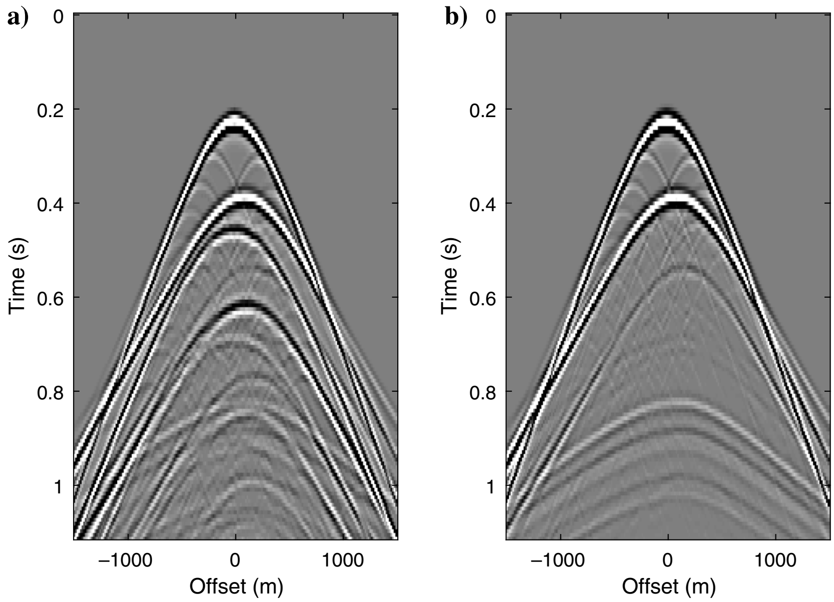

Figure 8. Modeled reference data. (a) True full wavefield after deghosting. (b) Reference primaries.

Field data example

We present an example of the proposed two-step framework applied to a North Sea data set from the Nelson field as shown in Figure 13, and a comprehensive investigation is shown in this section. The data are extracted from a 2D dual-sensor towed-streamer line with 25 m source spacing and 12.5 m receiver spacing. From the

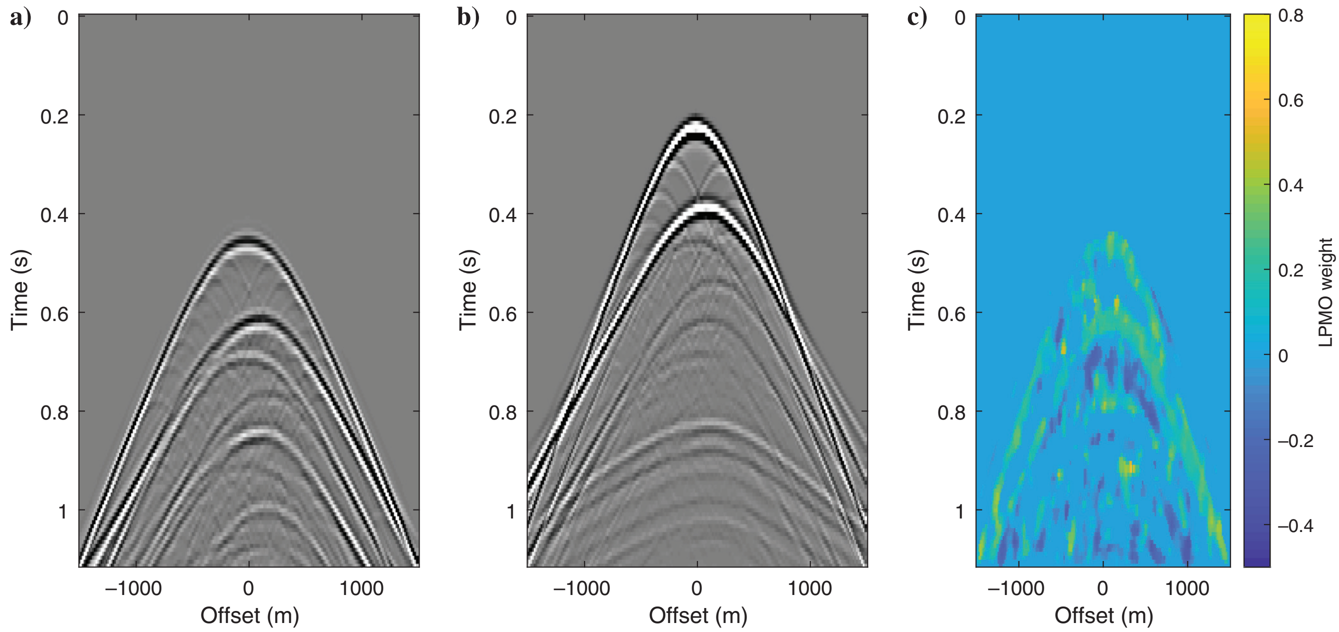

Figure 9. Initially predicted (a) multiples and (b) primaries using conservative SRME with a global subtraction window. (c) The estimated LPMO weight based on (a and b). The surface-related multiple leakage can be effectively detected by the LPMO weight. Note that the negative weights come from phase-shift errors during conservative SRME.

dual-sensor data, the upgoing wavefield is obtained (Cambois et al., 2009). By using reciprocity, shot interpolation, and near-offset reconstruction (Kabir and Verschuur, 1995), a split-spread data set is obtained, from which a fixed-spread subset is selected with 201 sources and 201 receivers. The source and receiver spacing is 12.5 m, where sources were interpolated from the original 25 m grid. The water depth is approximately 100 m, which is relatively shallow. The same data are used in Baardman et al. (2010) for inversion-type SRME. From Figure 13, it can be seen that surface-related multiples are clearly present and that the primaries are strongly interfered by the multiples.

Initially predicted multiples and primaries using conservative SRME with large local subtraction windows (500 ms $*$ 80 traces) are displayed in Figure 14a and 14b, respectively. The filter length is 20 ms. Due to the fact that 3D data can never be perfectly represented by a 2D theory and given unavoidable interpolation errors, surface-related multiple leakage is obvious in the initially predicted primary model. Besides, the shallow-water scenario makes the

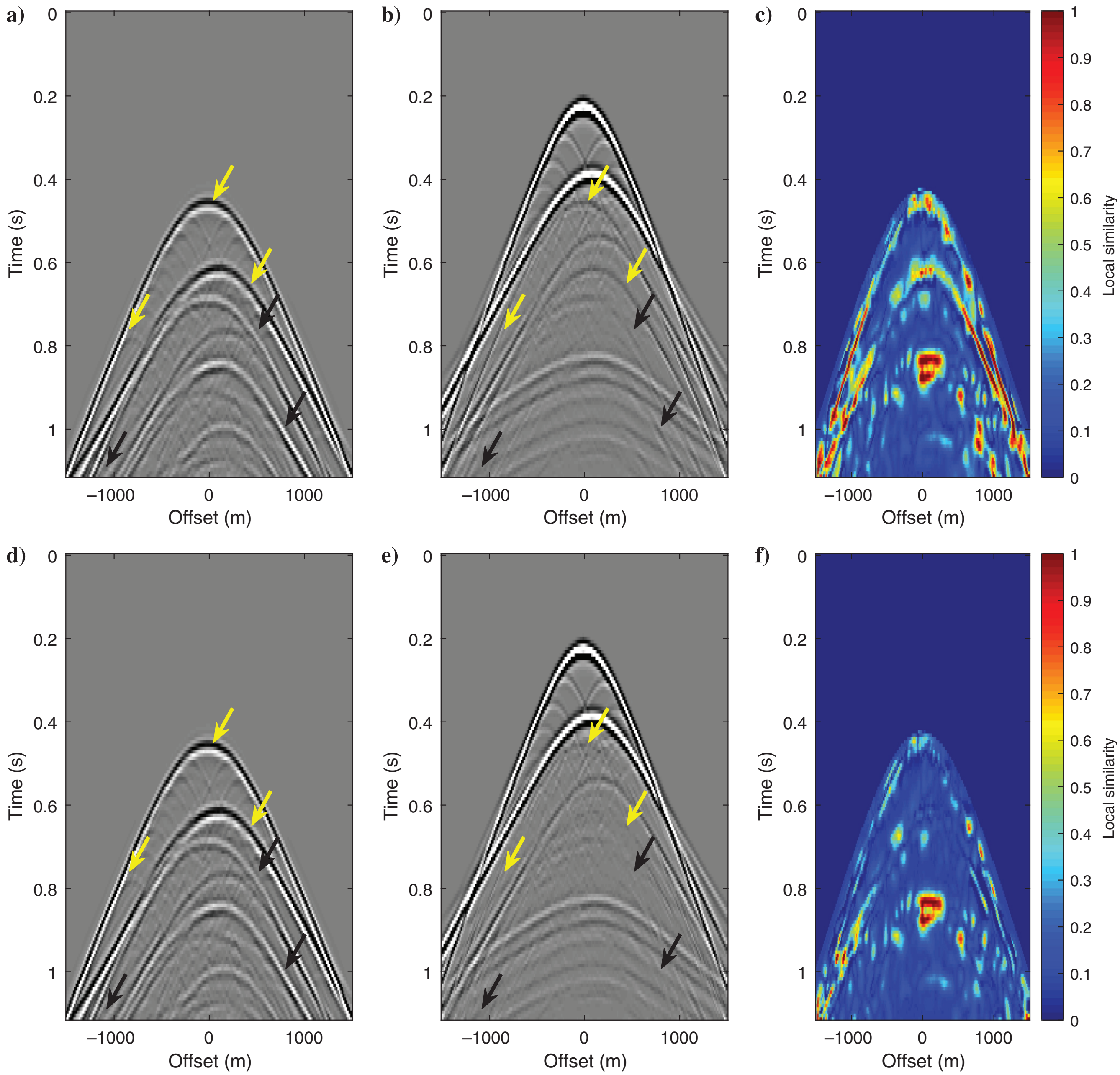

Figure 10. (a and b) Initially predicted multiples and primaries using conservative SRME with a global subtraction window, respectively. (d and e) Final estimated multiples and primaries after LPMO, respectively. (c and f) Local similarity maps before and after LPMO, respectively. The yellow arrows indicate where the leaked multiples are extracted, and the black arrows indicate where the phase-shift leaked multiples are extracted.

problem even more difficult. The proposed LPMO weight is displayed in Figure 14c, in which we are able to effectively detect the shape and position of the leaked multiples. In this example, the smoothing radius of the triangle smoothing operator is 2 time samples, the thresholding ranges from 0 to 1, and the size of the median filter is 3 time samples $*$ 3 traces. After LPMO, the final estimated multiples and primaries are presented in Figure 15. We are confident about the first-order surface-related multiple leakages indicated by the yellow arrows. Therefore, the most obvious multiple leakages at approximately 0.7 s are effectively extracted in the final primary model shown in Figure 15e, while we can also observe the final estimated multiples retrieved some of their leaked multiple energy shown in Figure 15d. Here, we also use local similarity maps to measure whether the leaked multiples are extracted or not. From the local similarity maps shown in Figure 15c and 15f, it can be seen that we have successfully extracted the leaked multiples especially at approximately 0.7 s. A detailed single-trace comparison at 87.5 m is shown in Figure 16. The blue line denotes the full wavefield, the green line denotes the conservative SRME primaries, and the red line denotes the primaries from the proposed framework. We can clearly see that the conservative SRME primar-

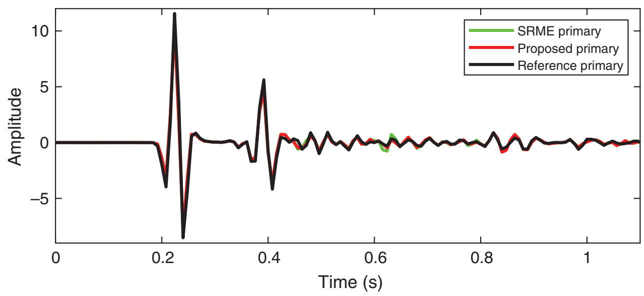

Figure 11. Single-trace comparison before and after LPMO. The black line denotes the reference primaries, the green line denotes the conservative SRME primaries, and the red line denotes the proposed primaries after LPMO.

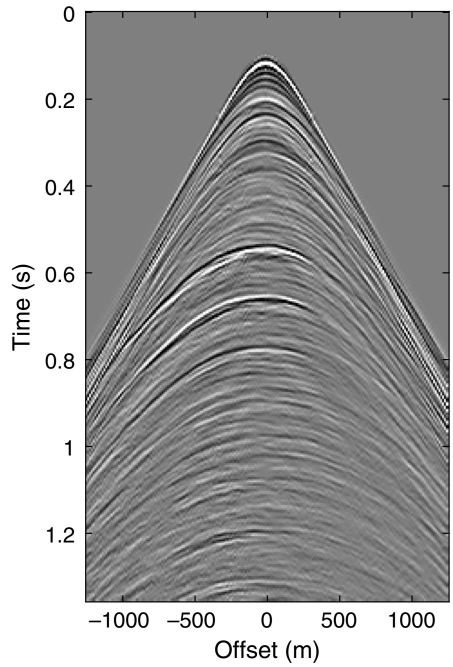

Figure 13. Field data shot record with surface-related multiples.

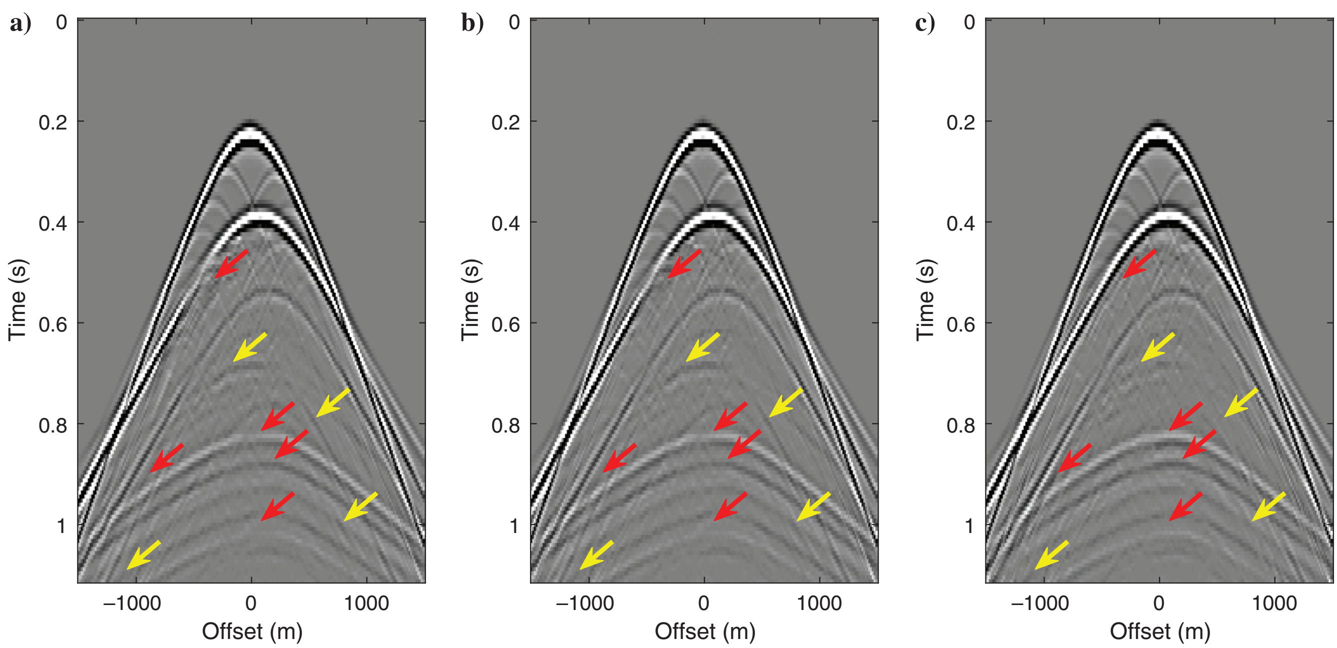

Figure 12. Comparison to the standard SRME. (a) $L2$-norm standard SRME primaries with a 320 ms $*$ 25 traces local subtraction window size. (b) $L1$-norm standard SRME primaries with a 320 ms $*$ 25 traces local subtraction window size. (c) The proposed primaries after LPMO (for comparison purposes). The yellow arrows in (a and b) denote the more severe multiple leakage compared to those in (c). The red arrows in (a and b) denote the primary damage compared to those in (c).

ies (the green line) at approximately 0.7 s contain strong leaked multiples that can be easily misinterpreted as primaries. After LPMO, the proposed primaries (the red line) at approximately 0.7 s become much smaller than the conservative SRME primaries (the green line). Similar observations can be made when selecting the −150 m common-offset gathers as presented in Figure 17. All of the yellow arrows in Figure 17b and 17c represent the improvement of the leaked multiples for the proposed framework. Moreover, a stacked section comparison before and after LPMO is provided in Figure 18 to demonstrate the effectiveness of the proposed method. Compared to the stacked section of the full wavefield shown in Figure 18a, the conservative SRME primaries in Figure 18b have already removed lots of multiple energy, but some amount of leaked multiples indicated by the yellow arrows are still there. After LPMO, the proposed primaries in Figure 18c display much less multiple leakage, which is better for accurate interpretation.

We also demonstrate the advantages of the proposed framework by providing a fair comparison with the standard SRME shot gathers and the stacked sections in Figure 19 and 20. The local subtraction window size is 160 ms $*$ 25 traces for standard SRME, and a longer filter length of 44 ms is used. From the shot gather comparison, it can be seen that the standard $L2$-norm SRME primaries in Figure 19a and the $L1$-norm SRME primaries in Figure 19b display slightly more multiple leakage than the proposed primaries indicated by the yellow arrows. Because of the small local subtraction windows and a long filter length, they are definitely better than the conservative SRME primaries shown in Figure 14b in terms of multiple leakage. Furthermore, the obvious primary damage indicated by the red arrows in the $L1$- and $L2$-norm standard SRME results reveals the overfitting of standard SRME, which can severely affect the subsequent imaging and interpretation accuracy. The standard SRME stacked sections in Figure 20a and 20b show the negative influences of the damaged primaries as indicated by the red arrows, in which the primary energy is dimmed in general compared to the proposed primaries in Figure 20c. Besides, the multiple leakage in the standard SRME results is still slightly more than that in the proposed results, as indicated by the yellow arrows, although it is already better than conservative SRME.

DISCUSSION

The essential differences between a one-point matching filter and the proposed LPMO step are more broadly discussed here including the computation of weights subject to smoothing, scaling, thresholding, and median filtering. First, the proposed framework can be considered as a one-point nonstationary matching filter, which is capable of adapting to the complex nonstationary seismic data. Second, obtaining a one-point nonstationary filter requires solving a highly underdetermined inverse problem. For this type of inverse problem, the shaping regularization is able to control the smoothness and deliver fast convergence, which is indicated by equation 9. The smoothing radius used in the constraint operator $\mathbf{S}(w)$ contributes to the final resolution of the estimated weights. Furthermore, the scaling parameter λ usually can be set as $\|\mathcal{M}^T\mathcal{M}\|_2^2$. The thresholding and median filtering operators in equation 10 are especially designed for the multiple leakage extraction problem, which is not needed for the random noise removal case. Thresholding of the estimated LPMO weights is highly necessary, due to the complex behavior of multiples and primaries, whereas median filtering is purely for obtaining a more stable result and avoiding outliers.

The thresholding range is the key parameter in the proposed framework. In the theory part, we mention that after shaping regularization, we obtain the estimated LPMO weights and then apply a thresholding operator $\mathbf{T}$ on the weights to force them to usually have values within 0 to 1. The logic behind it is shown in Figure 21. The yellow line indicates the estimated multiples from the conservative SRME. Usually, we can safely assume that the amplitude of the leaked multiple should be smaller than that of the estimated multi-

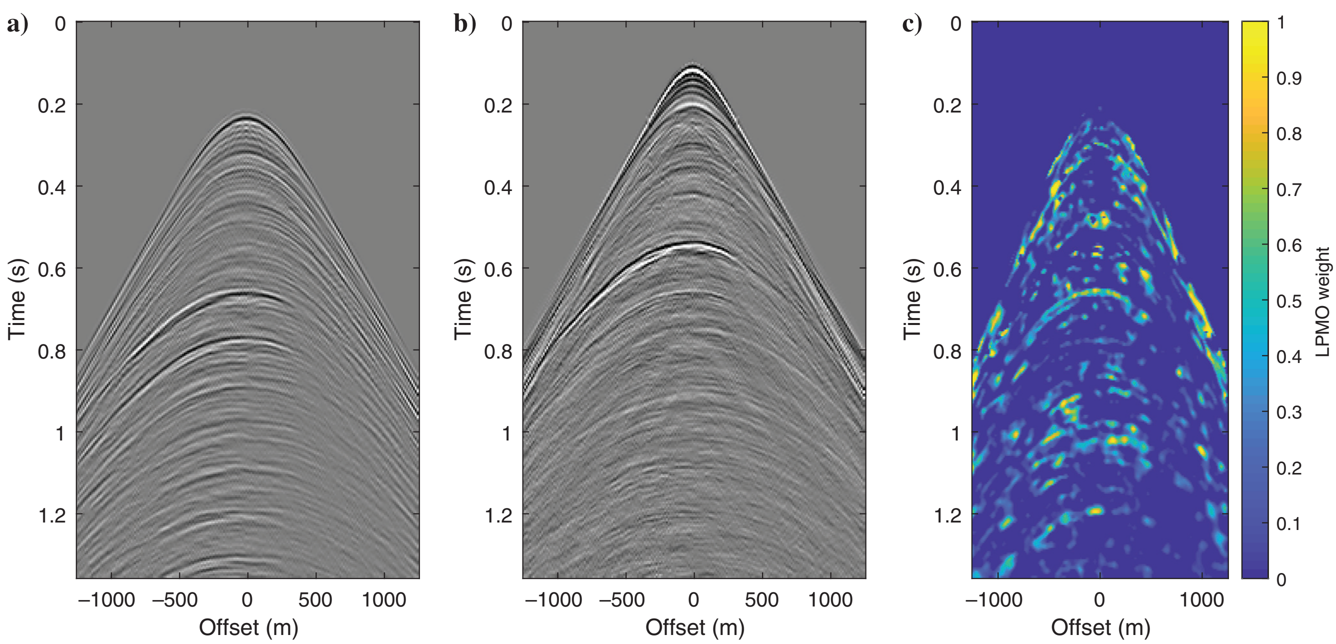

Figure 14. Initially estimated (a) multiples and (b) primaries using conservative SRME with large subtraction windows. (c) The estimated LPMO weight based on (a and b). The surface-related multiple leakage can be effectively detected by the LPMO weight.

ple, which means that the estimated weights should be smaller than 1. As mentioned before, the overall LPMO can be seen as a one-point nonstationary matching filter (Chen and Fomel, 2015) and the objective function only cares about the minimum energy after matching and subtraction. More importantly, the algorithm itself cannot tell the difference between leaked multiples and primaries. Therefore, there is a tendency for the algorithm to use estimated multiples to match the primaries, which will result in quite large weights (i.e., $\mathbf{w} > 1$) due to the fact that primaries usually have a much higher amplitude than the estimated multiples. Thus, a thresholding operator can help the algorithm focus on the leaked multiple energy of interest. It is necessary to be aware of other special situations regarding the thresholding operator. First, as mentioned in the complex salt model example, the estimated LPMO weight introduces some negative values as shown in Figure 9c. This is because of phase-shift errors when predicting the multiple model. Thus, in this case, the multiple leakage and the estimated multiple model might have opposite polarity, which can be compensated by introducing negative weights. Second, real data always have some sampling issues (e.g., near offsets missing and crossline undersampling). Even the most advanced interpolation approaches still bring some reconstruction errors to the data, and then those errors

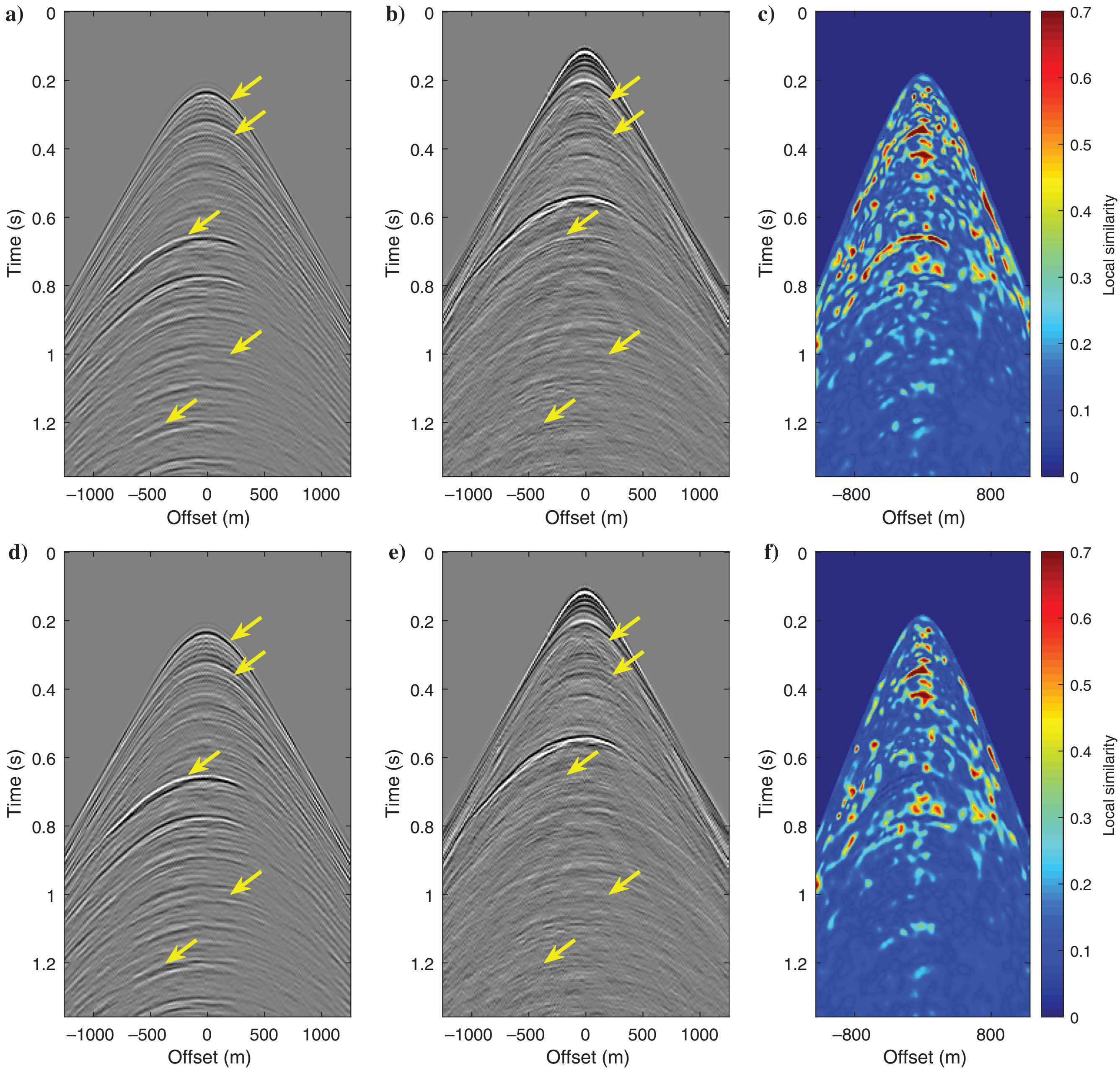

Figure 15. (a and b) Initially predicted multiples and primaries using conservative SRME with large subtraction windows, respectively. (d and e) Final estimated multiples and primaries after LPMO, respectively. (c and f) Local similarity maps before and after LPMO, respectively. The yellow arrows indicate where the leaked multiples are extracted.

might result in the relatively weaker amplitude of the predicted multiples. Therefore, combined with phase-shift errors and 2D/3D effects, there might be a chance that the estimated multiples are weaker than the multiple leakage. Weights larger than 1 can then be tested to determine the performance. Based on our experience, the robust range for the thresholding operator $\mathbf{T}$ is between 0 and 1. When there are still some obvious phase-shift multiple leakage left, the range can be revised to between -0.5 and 1. For the field data set, the upper limit of the thresholding operator should be smaller than 2 based on our experience.

Smoothing is also an important part in shaping regularization. In this paper, the triangle smoothing operator is used in shaping regularization-based inversion. The sampling in time for the lens-shaped model and field data is 4 ms, whereas the sampling for the complex salt model is 8 ms. The smoothing radius of the triangle smoothing operator for all of the examples is set as 2 time samples for higher resolution. The range for smoothing radius based on our experiences can range from 2 to 10 time samples depending on the desired resolution.

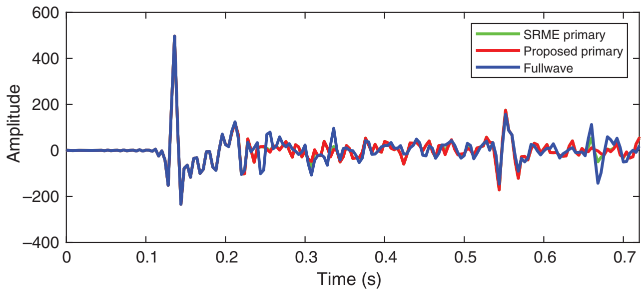

Figure 16. Single-trace comparison at offset 87.5 m before and after LPMO. The blue line denotes the full wavefield, the green line denotes the conservative SRME primaries, and the red line denotes the proposed primaries after LPMO.

The proposed framework is still based on the basic assumption that the primaries and multiples should not correlate. Thus, it is worth noting that some red areas in the local similarity maps are unchanged before and after LPMO. These high-similarity areas indicate where the multiples and primaries are highly correlated and overlapped, which violates the initial assumption of most adaptive subtraction methods. Therefore, most methods in the literature fail to correctly extract the leakage if it exists in these areas. For our proposed approach, its multiple leakage extraction power is within the limitation of the orthogonal assumption. However, if the conservative primary estimation (e.g., the conservative SRME) is used and followed by LPMO in our proposed framework, the primary damage can be kept to a minimum compared to other standard methods.

As for the computational time consumption, it depends on the actual situations and is relatively difficult to compare. In general, most time consumption for the standard SRME comes from the parameter tuning of the adaptive subtraction. Practitioners have to test a set of different window sizes and filter lengths to find the desired optimal setting, which is usually a tedious process. Besides, some amount of time is required to compare different results and the trade-off between multiple leakage and primary damage has to be decided by the practitioners. Therefore, all of the parameter tuning-related time consumption is hard to estimate. As for the proposed framework, the LPMO definitely takes some extra time for inversion (e.g., it is approximately 10 times more expensive for the field data example), but it saves practitioners time from fine-tuning the parameters. Above all, we could also consider the LPMO as an extra QC step to evaluate whether the multiple energy is leaked or not.

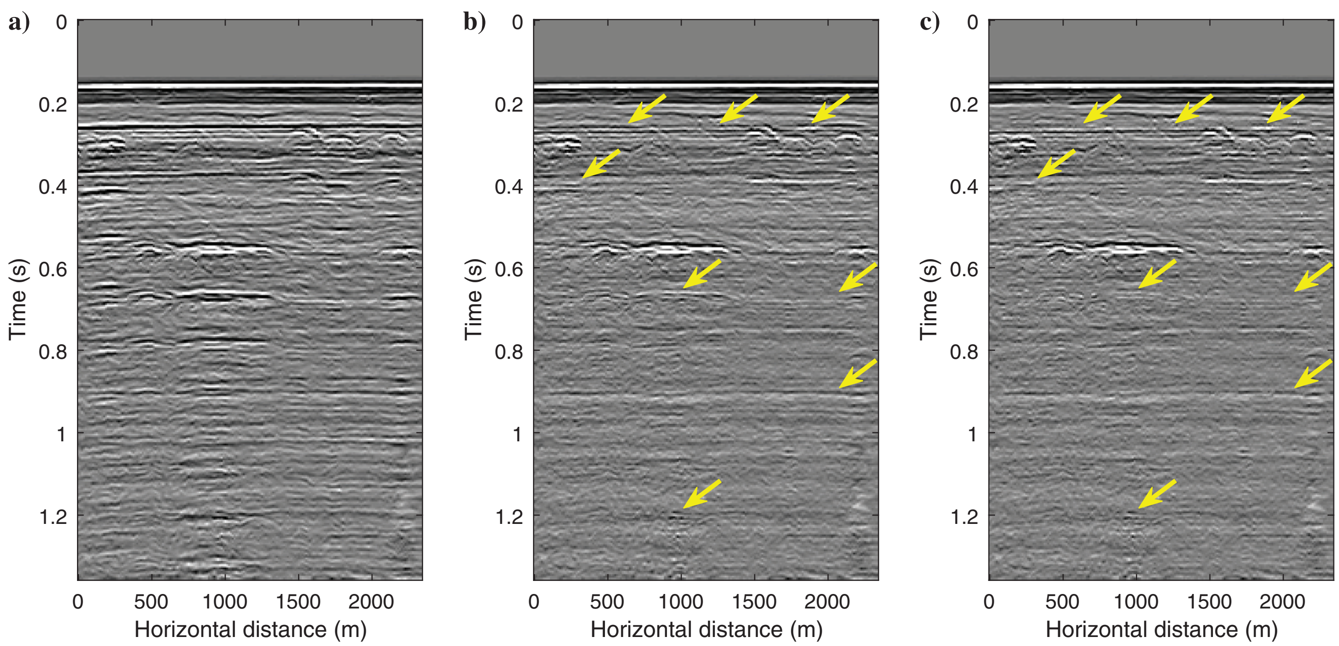

Figure 17. Common-offset gather comparison at offset −150 m. (a) Common-offset gather of the input. (b) Common-offset gather of the initially predicted primaries by conservative SRME with large subtraction windows. (c) Common-offset gather of the final estimated primaries after LPMO.

From almost-perfect-world synthetic examples, the leaked surface-related multiples may not seem to have strong influences on primaries due to the relatively small amplitude. However, real-world field data with 2D/3D effects and interpolation errors always tend to show much more obvious and severe surface-related multiple leakage. The proposed two-step framework thus can be a quite helpful toolbox to attack the multiple leakage without damaging primaries. Meanwhile, it can also be regarded as another tool in the toolbox of various multiple prediction and subtraction techniques.

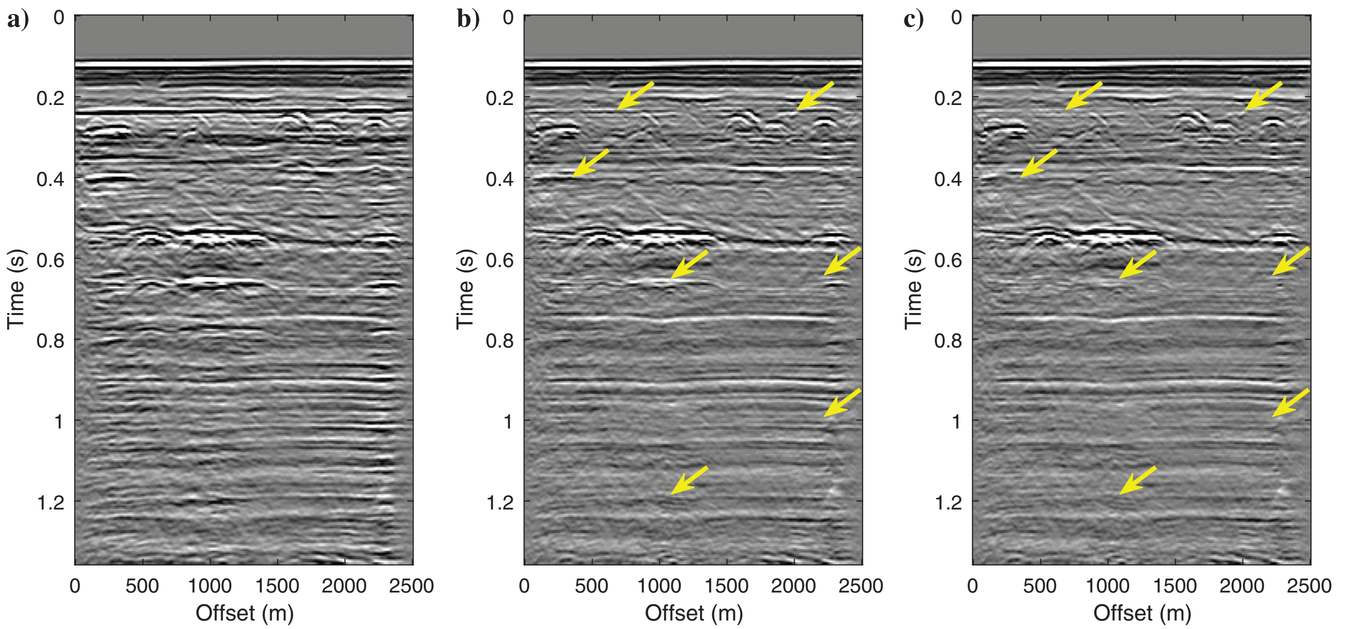

Figure 18. Stacked section comparison. (a) Stacked section of the input. (b) Stacked section of the initially predicted primaries by conservative SRME with large subtraction windows. (c) Stacked section of the final estimated primaries after LPMO.

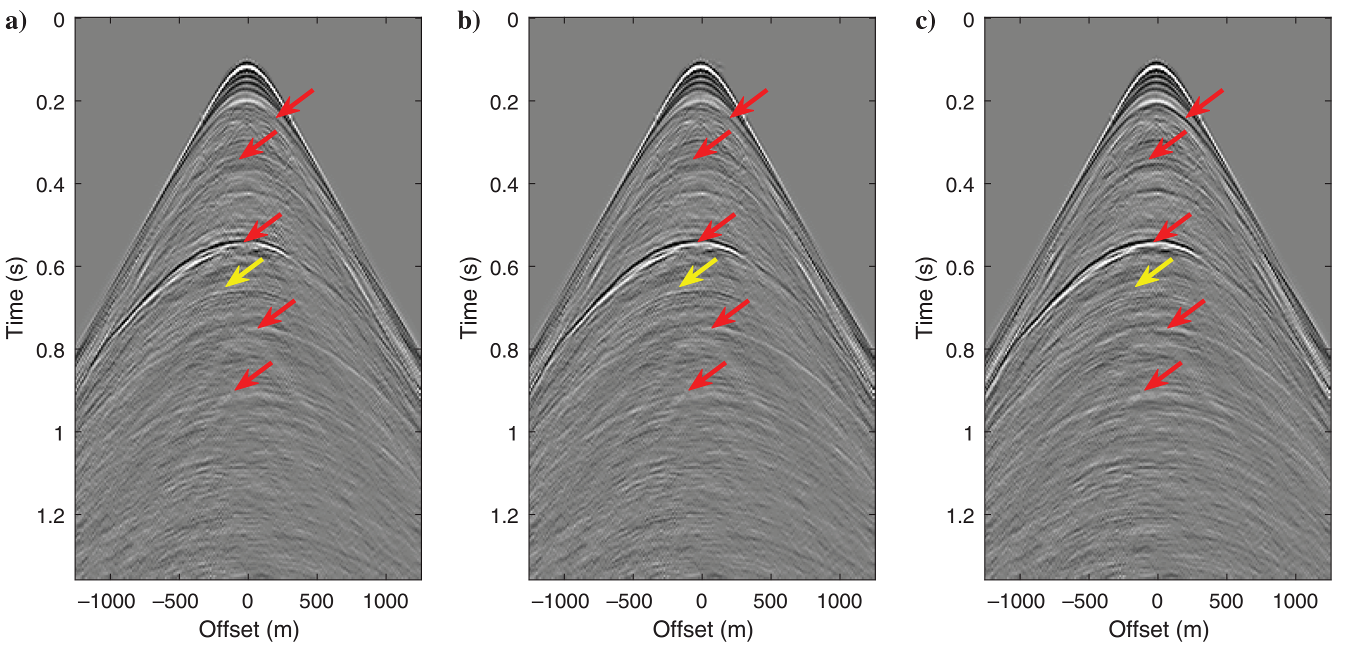

Figure 19. Shot gather comparison to standard SRME. (a) $L2$-norm standard SRME primaries with a 160 ms $*$ 25 traces local subtraction window size. (b) $L1$-norm standard SRME primaries with a 160 ms $*$ 25 traces local subtraction window size. (c) The proposed primaries after LPMO (for comparison purposes). The yellow arrows in (a and b) denote the more severe multiple leakage compared to those in (c). The red arrows in (a and b) denote more primary damage compared to those in (c).

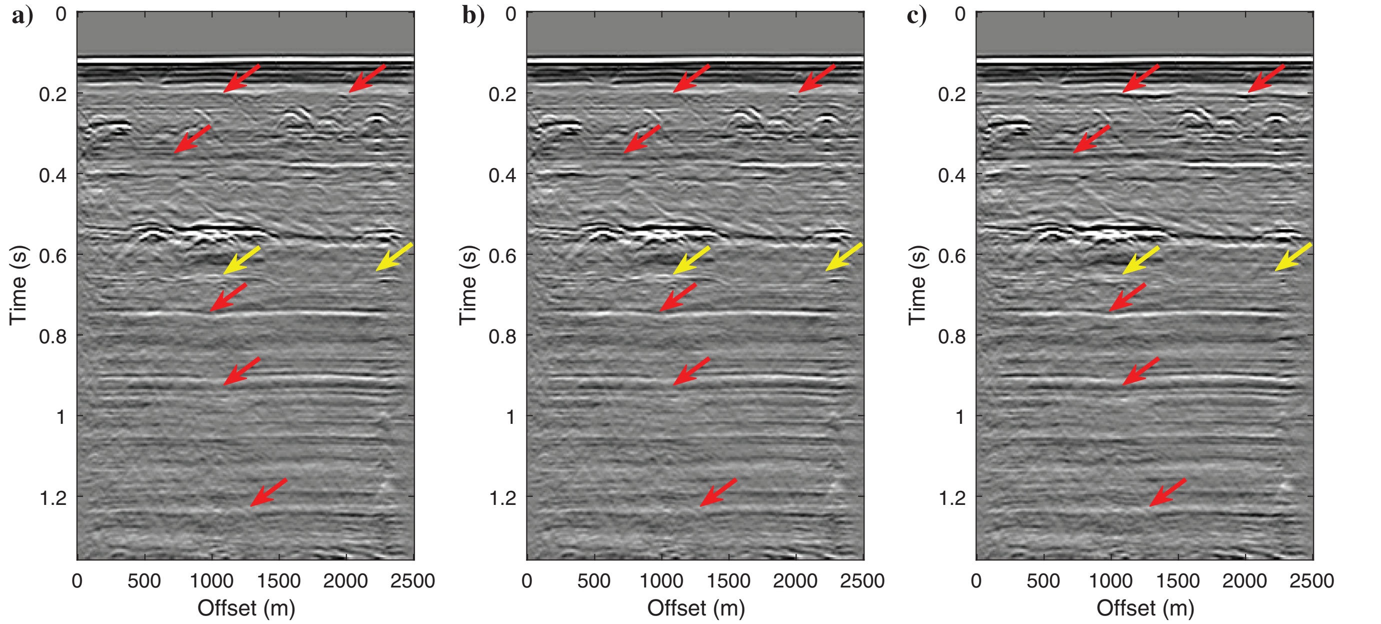

Figure 20. Stacked section comparison to the standard SRME. (a) Stacked section of the $L2$-norm standard SRME primaries with a 160 ms $*$ 25 traces local subtraction window size. (b) Stacked section of the $L1$-norm standard SRME primaries with a 160 ms $*$ 25 traces local subtraction window size. (c) Stacked section of the final estimated primaries after LPMO. The yellow arrows in (a and b) denote more severe multiple leakage compared to those in (c). The red arrows in (a and b) denote more primary damage compared to those in (c).

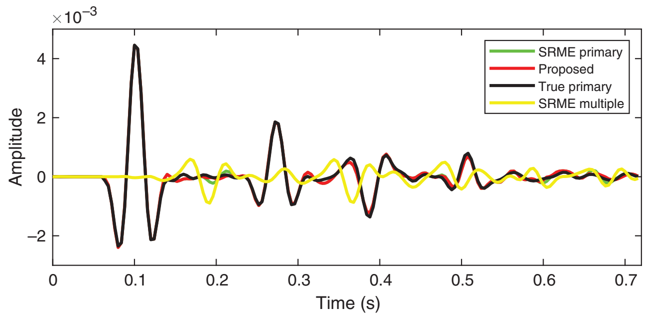

Figure 21. Single-trace comparison before and after LPMO from the lens-shaped synthetic model.

For very complex field data, extracting leaked multiples in the shot domain might not be enough, therefore, multidomain LPMO is suggested (Zhang et al., 2019b). The common-offset domain is an appropriate choice, in which we might observe the leakage with less effort. The whole framework is exactly the same as the shot-domain extraction based on LPMO. The only difference is to sort the data to the common-offset domain in advance.

Our proposed two-step framework based on LPMO aims to solve the surface-related multiple leakage problem for all of the existing primary and multiple estimation approaches. That is, as long as there is multiple leakage in the estimated primary model, our proposed LPMO can be attached to any primary estimation approach. For example, more advanced inversion-based CL-SRME or EPSI is, to some extent, able to alleviate the multiple leakage problem, but it may still suffer from such multiple leakage, especially for complex coarsely sampled field data with 2D/3D effects. Therefore, we can regard either CL-SRME or EPSI as our primary estimation engine for the initial step, and then the second step, LPMO, as a remedy can be applied to extract the leaked multiples. Moreover, model-driven multiple prediction approaches (e.g., model-based water-layer demultiple [Wang et al., 2011]) can also be attached by the proposed LPMO step as long as the adaptive subtraction is involved.

Currently, there is no requirement of broadband data for our proposed framework. In terms of the leakage as a function of frequency, a possible solution might be that the low-frequency components can be processed with large local windows in the adaptive subtraction, whereas the high-frequency components can be processed with smaller local windows. The proposed LPMO step could be further applied to low- and high-frequency components with different parameter settings. Further research is needed to investigate this issue in detail.

CONCLUSION

We have introduced a new two-step framework for surface-related multiple leakage extraction, and we thus obtain a better estimated primary model. This two-step framework using LPMO is highly efficient for leaked multiple extraction and can work for various multiple prediction methods. Conservative SRME is used as the initial estimation step followed by LPMO as the remedy to correct the estimated primaries and multiples. Applications to two synthetic data sets and one field data set demonstrate the good performance of the proposed framework for primary estimation compared with the standard SRME results.

ACKNOWLEDGMENTS

The authors would like to thank the editor J. Shragge for improving this paper in the final phase, and we also thank the associate editor B. Witten, C. Kostov, and two other anonymous reviewers for their insightful suggestions. D. Zhang, S. Qu, and D. J. Verschuur thank the sponsors of the Delphi Consortium for their support. Y. Chen is supported by the Thousand Youth Talents Plan of China and the Starting Funds from Zhejiang University. The authors would also like to thank PGS for providing the Nelson field data.

DATA AND MATERIALS AVAILABILITY

Data associated with this research are available and can be obtained by contacting the corresponding author.

REFERENCES

Baardman, R. H., D. J. Verschuur, R. G. van Borselen, M. O. Frijlink, and R. F. Hegge, 2010, Estimation of primaries by sparse inversion using dual-sensor data: 80th Annual International Meeting, SEG, Expanded Abstracts, 3468–3472, doi: 10.1190/1.3513569.

Berkhout, A. J., 1982, Seismic migration, imaging of acoustic energy by wavefield extrapolation, A: Theoretical aspects, 2nd ed.: Elsevier.

Berkhout, A. J., 2014, Review paper: An outlook on the future of seismic imaging — Part 1: Forward and reverse modelling: Geophysical Prospecting, **62**, 911–930, doi: 10.1111/1365-2478.12161.

Berkhout, A. J., and D. J. Verschuur, 1997, Estimation of multiple scattering by iterative inversion — Part 1: Theoretical considerations: Geophysics, **62**, 1586–1595, doi: 10.1190/1.1444261.

Brown, M. P., and A. Guitton, 2005, Least-squares joint imaging of multiples and primaries: Geophysics, **70**, no. 5, S79–S89, doi: 10.1190/1.2052471.

Cambois, G., D. Carlson, C. Jones, M. Lesnes, W. Söllner, H. Tabti, and A. Day, 2009, Dual-sensor streamer data, acquisition QC and attenuation of seismic interferences and other noises: 71st Annual International Conference and Exhibition, EAGE, Extended Abstracts, X033, doi: 10.3997/2214-4609.201400517.

Chen, W., J. Xie, S. Zu, S. Gan, and Y. Chen, 2017, Multiple reflections noise attenuation using adaptive randomized-order empirical mode decomposition: IEEE Geoscience and Remote Sensing Letters, **14**, 18–22, doi: 10.1109/LGRS.2016.2622918.

Chen, Y., 2015, Iterative deblending with multiple constraints based on shaping regularization: IEEE Geoscience and Remote Sensing Letters, **12**, 2247–2251, doi: 10.1109/LGRS.2015.2463815.

Chen, Y., and S. Fomel, 2015, Random noise attenuation using local signal-and-noise orthogonalization: Geophysics, **80**, no. 6, WD1–WD9, doi: 10.1190/geo2014-0227.1.

Chen, Y., W. Huang, Y. Zhou, W. Liu, and D. Zhang, 2018, Plane-wave orthogonal polynomial transform for amplitude-preserving noise attenuation: Geophysical Journal International, **214**, 2207–2223, doi: 10.1093/gji/ggy267.

Chen, Y., S. Jiao, J. Ma, H. Chen, Y. Zhou, and S. Gan, 2015, Ground-roll noise attenuation using a simple and effective approach based on local band-limited orthogonalization: IEEE Geoscience and Remote Sensing Letters, **12**, 2316–2320, doi: 10.1109/LGRS.2015.2475280.

Davydenko, M., and D. J. Verschuur, 2017, Full wavefield migration: Using surface and internal multiples: Geophysical Prospecting, **65**, 7–21, doi: 10.1111/1365-2478.12360.

Davydenko, M., and D. J. Verschuur, 2018, Including and using internal multiples in closed-loop imaging — Field data examples: Geophysics, **83**, no. 4, R297–R305, doi: 10.1190/geo2017-0533.1.

Dragoset, B., E. Verschuur, I. Moore, and R. Bisley, 2010, A perspective on 3D surface-related multiple elimination: Geophysics, **75**, no. 5, 75A245–75A261, doi: 10.1190/1.3475413.

Dragoset, W. H., and Z. Jericevic, 1998, Some remarks on surface multiple attenuation: Geophysics, **63**, 772–789, doi: 10.1190/1.1444377.

Fomel, S., 2007a, Local seismic attributes: Geophysics, **72**, no. 3, A29–A33, doi: 10.1190/1.2437573.

Fomel, S., 2007b, Shaping regularization in geophysical-estimation problems: Geophysics, **72**, no. 2, R29–R36, doi: 10.1190/1.2433716.

Fomel, S., 2009, Adaptive multiple subtraction using regularized nonstationary regression: Geophysics, **74**, no. 1, V25–V33, doi: 10.1190/1.3043447.

Gülünay, N., 2017, Signal leakage in f-x deconvolution algorithms: Geophysics, **82**, no. 5, W31–W45, doi: 10.1190/geo2017-0007.1.

Guitton, A., 2005, Multiple attenuation in complex geology with a pattern-based approach: Geophysics, **70**, no. 4, V97–V107, doi: 10.1190/1.1997369.

Guitton, A., and D. J. Verschuur, 2004, Adaptive subtraction of multiples using the L1-norm: Geophysical Prospecting, **52**, 27–38, doi: 10.1046/j.1365-2478.2004.00401.x.

Hampson, D., 1986, Inverse velocity stacking for multiple elimination: Canadian Journal of Exploration Geophysics, **22**, 44–55.

Hanafy, S. M., and G. T. Schuster, 2014, Interferometric interpolation of sparse marine data: Geophysical Prospecting, **62**, 1–16, doi: 10.1111/1365-2478.12066.

Hargreaves, N., 2006, Surface multiple attenuation in shallow water and the construction of primaries from multiples: 76th Annual International Meeting, SEG, Expanded Abstracts, 2689–2693, doi: 10.1190/1.2370080.

Hermann, F. J., and D. J. Verschuur, 2004, Curvelet-domain multiple elimination with sparseness constraints: 74th Annual International Meeting, SEG, Expanded Abstracts, 1333–1336, doi: 10.1190/1.1851110.

Hermann, F. J., D. Wang, and D. J. Verschuur, 2008, Adaptive curvelet-domain primary-multiple separation: Geophysics, **73**, no. 3, A17–A21, doi: 10.1190/1.2904986.

Hung, B., M. Wang, K. Yang, and X. Wu, 2014, Enhanced internal multiple attenuation in shallow water environment: 84th Annual International Meeting, SEG, Expanded Abstracts, 4147–4151, doi: 10.1190/segam2014-0276.1.

Jin, H., and P. Wang, 2012, Model-based water-layer demultiple (MWD) for shallow water: From streamer to OBS: 82nd Annual International Meeting, SEG, Expanded Abstracts, doi: 10.1190/segam2012-1401.1.

Kabir, M. M. N., and D. J. Verschuur, 1995, Restoration of missing offsets by parabolic Radon transform: Geophysical Prospecting, **43**, 347–368, doi: 10.1111/j.1365-2478.1995.tb00257.x.

Kelamis, P. G., and D. J. Verschuur, 2000, Surface-related multiple elimination on land seismic data — Strategies via case studies: Geophysics, **65**, 719–734, doi: 10.1190/1.1444771.

Kostov, C., F. X. de Melo, A. Raj, A. Zarkhidze, A. Cooke, G. Miers, and J. Bacon, 2015, Multiple attenuation for shallow-water surveys: Notes on old challenges and new opportunities: The Leading Edge, **34**, 760–768, doi: 10.1190/tle34070760.1.

Lin, T. T. Y., and F. J. Herrmann, 2013, Robust estimation of primaries by sparse inversion via one-norm minimization: Geophysics, **78**, no. 3, R133–R150, doi: 10.1190/geo2012-0097.1.

Lopez, G. A., and D. J. Verschuur, 2014, Closed-loop SRME — A new direction in surface multiple removal algorithms: 76th Annual International Conference and Exhibition, EAGE, Extended Abstracts, We E102 02, doi: 10.3997/2214-4609.20141033.

Lopez, G. A., and D. J. Verschuur, 2015, Closed-loop surface-related multiple elimination and its application to simultaneous data reconstruction: Geophysics, **80**, no. 6, V189–V199, doi: 10.1190/geo2015-0287.1.

Lu, S., D. N. Whitmore, A. A. Valenciano, and N. Chemingui, 2015, Separated-wavefield imaging using primary and multiple energy: The Leading Edge, **34**, 770–778, doi: 10.1190/tle34070770.1.

Nath, A., and D. J. Verschuur, 2017, Using surface-related multiples in imaging for data with large acquisition gaps: 87th Annual International Meeting, SEG, Expanded Abstracts, 4768–4772, doi: 10.1190/segam2017-17794146.1.

Neelamani, R., A. Baumstein, and W. S. Ross, 2010, Adaptive subtraction using complex-valued curvelet transforms: Geophysics, **75**, no. 4, V51–V60, doi: 10.1190/1.3453425.

Ryu, J. V., 1982, Decomposition (DECOM) approach applied to wave field analysis with seismic reflection records: Geophysics, **47**, 869–883, doi: 10.1190/1.1441354.

Spitz, S., 1999, Pattern recognition, spatial predictability, and subtraction of multiple events: The Leading Edge, **18**, 55–58, doi: 10.1190/1.1438154.

van Dedem, E. J., and D. J. Verschuur, 2005, 3D surface-related multiple prediction — A sparse inversion approach: Geophysics, **70**, no. 3, V31–V43, doi: 10.1190/1.1925752.

van Groenestijn, G. J. A., and D. J. Verschuur, 2009a, Estimating primaries by sparse inversion and application to near-offset data reconstruction: Geophysics, **74**, no. 3, A23–A28, doi: 10.1190/1.3111115.

van Groenestijn, G. J. A., and D. J. Verschuur, 2009b, Estimation of primaries and near offsets by sparse inversion: Marine data applications: Geophysics, **74**, no. 6, R119–R128, doi: 10.1190/1.3213532.

Verschuur, D. J., 2006, Seismic multiple removal techniques — Past, present and future: EAGE Publications BV.

Verschuur, D. J., and A. J. Berkhout, 1997, Estimation of multiple scattering by iterative inversion — Part 2: Practical aspects and examples: Geophysics, **62**, 1596–1611, doi: 10.1190/1.1444262.

Verschuur, D. J., A. J. Berkhout, and C. P. A. Wapenaar, 1992, Adaptive surface-related multiple elimination: Geophysics, **57**, 1166–1177, doi: 10.1190/1.1443330.

Wang, D., R. Saab, O. Yilmaz, and F. J. Hermann, 2008, Bayesian wavefield separation by transform-domain sparsity promotion: Geophysics, **73**, no. 5, A33–A38, doi: 10.1190/1.2952571.

Wang, P., H. Jin, S. Xu, and Y. Zhang, 2011, Model-based water-layer demultiple: 81st Annual International Meeting, SEG, Expanded Abstracts, 3551–3555, doi: 10.1190/1.3627937.

Wang, Y., Y. Luo, and G. T. Schuster, 2009, Interferometric interpolation of missing seismic data: Geophysics, **74**, no. 3, SI37–SI45, doi: 10.1190/1.3110072.

Weglein, A. B., F. A. Gasparotto, P. M. Carvalho, and R. H. Stolt, 1997, An inverse-scattering series method for attenuating multiples in seismic reflection data: Geophysics, **62**, 1975–1989, doi: 10.1190/1.1444298.

Xue, Y., J. Yang, J. Ma, and Y. Chen, 2016, Amplitude-preserving nonlinear adaptive multiple attenuation using the high-order sparse Radon transform: Journal of Geophysics and Engineering, **13**, 207–219, doi: 10.1088/1742-2132/13/3/207.

Zhang, D., and G. T. Schuster, 2013, Least-squares reverse time migration of multiples: Geophysics, **79**, no. 1, S11–S21, doi: 10.1190/geo2013-0156.1.

Zhang, D., and E. Verschuur, 2019, Integration of closed-loop surface-related multiple estimation and full wavefield migration for shallow water: 81st Annual International Conference and Exhibition, EAGE, Extended Abstracts, Tu_R01_03, doi: 10.3997/2214-4609.201900779.

Zhang, D., E. Verschuur, and Y. Chen, 2019a, Surface multiple leakage extraction using local primary-and-multiple orthogonalization: 81st Annual International Conference and Exhibition, EAGE, Extended Abstracts, We_R06_06, doi: 10.3997/2214-4609.201901199.

Zhang, D., E. Verschuur, S. Qu, and Y. Chen, 2019b, Multi-domain surface multiple leakage extraction using local primary-and-multiple orthogonalization: 89th Annual International Meeting, SEG, Expanded Abstracts, 4585–4589, doi: 10.1190/segam2019-3216199.1.